

ChemComm

Accepted Manuscript



This article can be cited before page numbers have been issued, to do this please use: H. Zhang, J. Li, Y. Chai, W. V. Wang, Z. Shi and Z. Xu, *Chem. Commun.*, 2017, DOI: 10.1039/C7CC01973D.



This is an Accepted Manuscript, which has been through the Royal Society of Chemistry peer review process and has been accepted for publication.

Accepted Manuscripts are published online shortly after acceptance, before technical editing, formatting and proof reading. Using this free service, authors can make their results available to the community, in citable form, before we publish the edited article. We will replace this Accepted Manuscript with the edited and formatted Advance Article as soon as it is available.

You can find more information about Accepted Manuscripts in the [author guidelines](#).

Please note that technical editing may introduce minor changes to the text and/or graphics, which may alter content. The journal's standard [Terms & Conditions](#) and the ethical guidelines, outlined in our [author and reviewer resource centre](#), still apply. In no event shall the Royal Society of Chemistry be held responsible for any errors or omissions in this Accepted Manuscript or any consequences arising from the use of any information it contains.



Journal Name

COMMUNICATION

Pyrazine-Fused Isoindigo: A New Building Block for Polymer Solar Cells with High Open Circuit Voltage

Received 00th January 20xx,
Accepted 00th January 20xxJiu-Long Li, Yun-Fei Chai, Wei Vanessa Wang, Zi-Fa Shi, Zhu-Guo Xu, Hao-Li Zhang^{a,b*}

DOI: 10.1039/x0xx00000x

www.rsc.org/

Pyrazine-fused isoindigo (PzIIG) was designed and synthesized as a novel electron-acceptor to construct two D-A conjugated polymers, PzIIG-BDT2TC8 and PzIIG-BTT2TC10. Both polymers were successfully applied in polymer solar cells, and the PzIIG-BDT2TC8 based solar cell device exhibited a PCE of 5.26 % with a high V_{oc} over 1.0 V.

Donor-acceptor (D-A) conjugated polymers have attracted great interest in recent years due to their applications in organic field effect transistors (OFETs)¹ and polymer solar cells (PSCs).² Organic optoelectronic devices based on D-A conjugated polymers possess some attracting characteristics, such as low cost fabrication, light-weight and flexibility.³ Recently, new electron-deficient units have been developed for the construction of D-A copolymers, such as the double B-N bridged bipyridyl (BNBP)^{4,5} and several lactam based electron-acceptors, including diketopyrrolopyrrole (DPP)⁶ and isoindigo (IIG).⁷

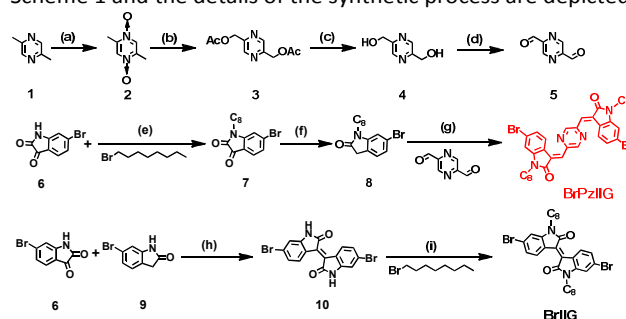
IIG is identified as one of the most efficient electron-withdrawing units to construct D-A conjugated polymers, due to its large optical transition dipole moment, strong electron-deficient characteristic and broad UV-vis absorption. IIG-based D-A conjugated polymers usually possess strong intramolecular charge transfer (ICT)⁸ and low optical band gap, which are beneficial for charge transport and light absorption.

However, the structure of IIG is not perfect for organic semiconductors. Steric-hindrance between the carbonyl oxygen of the oxindole and the proton on the phenyl ring makes the IIG unit slightly twisted from the desired planar conformation.⁹ Ashraf's group replaced the phenyl rings in IIG with thiophene and synthesized thienoisindigo (TIIG) to

achieve better planarity.¹⁰ Several TIIG based conjugated copolymer exhibited enhanced mobility in field effect transistors,^{8,11} suggesting the important role of planarity for charge transport in conjugated copolymers.

In this communication, we report a novel pyrazine-fused isoindigo (named as PzIIG) unit, which possesses more planar structure and stronger electron-withdrawing characteristic compared with IIG. The PzIIG unit contains one pyrazine ring inserted in the middle of the IIG. The pyrazine unit plays two roles. First, pyrazine ring could form intramolecular hydrogen bonding with the nearby phenyl unit to improve the molecular planarity and rigidity, providing longer effective conjugation length compared with IIG. Second, the pyrazine ring acts as a strong electron deficient unit to improve the electron-withdrawing ability. Given the more electron deficient nature of pyrazine than thiophene, the PzIIG shall be a stronger electron acceptor unit than TIIG. To demonstrate capability of PzIIG as an efficient electron-withdrawing unit, two D-A conjugated polymers, PzIIG-BDT2TC8 and PzIIG-BTT2TC10, were synthesized and applied in PSCs successfully. The PzIIG-BDT2TC8 based PSCs showed a PCE of 5.26 % with a high V_{oc} up to 1.01 V.

The synthesis of the key building block brominated pyrazine-fused isoindigo (named as BrPzIIG) is illustrated in Scheme 1 and the details of the synthetic process are depicted



Scheme 1 Synthetic routes of BrPzIIG and BrIIG : (a) m-CPBA, EA, R.T., 24h, (b) Ac₂O, reflux, 24h, (c) MeONa, MeOH, R.T., 3h, (d) MnO₂, Dioxane, reflux, 1h, (e) DMF, K₂CO₃, 80 °C, 2h, (f) TiCl₄/Zn, THF, (g) piperidine, EtOH, 80 °C, 24 h, (h) acetic acid, HCl, reflux, 24h, (i) DMF, K₂CO₃, 80 °C, 2h.

^a State Key Laboratory of Applied Organic Chemistry (SKLAOC); Key Laboratory of Special Function Materials and Structure Design (MOE); College of Chemistry and Chemical Engineering, Lanzhou University, Lanzhou, 730000, P. R. China E-mail: haoli.zhang@lzu.edu.cn

^b Tianjin Key Laboratory of Molecular Optoelectronic Sciences, Department of Chemistry, Tianjin University, and Collaborative Innovation Center of Chemical Science and Engineering (Tianjin), Tianjin 300072, P. R. China

†Electronic Supplementary Information (ESI) available: Experimental details, DFT calculations, CV, TGA, SCLC, AFM and NMR spectra. See DOI: 10.1039/x0xx00000x

COMMUNICATION

Journal Name

in Electronic Supplementary Information (ESI[†]). Pyrazine-2,5-dialdehyde was obtained through four steps,¹² which was the most important intermediate molecule. Meanwhile, the octyl unit was introduced in the 6-bromoisatin and one carbonyl group was selectively reduced to obtain the alkylated 6-bromoindolin-2-one. Then the pyrazine-2,5-dialdehyde and alkylated 6-bromoindolin-2-one were used as substrates for Knoevenagel condensations under alkaline condition to give the **BrPzIIG**. For comparison purpose, brominated isoindigo (named as **BrIIG**) was also synthesized, the synthetic procedure is illustrated in Scheme 1 and the details are depicted in ESI. The **BrPzIIG** exhibits good solubility in common organic solvents such as dichloromethane, chloroform and ethyl acetate, making it an ideal reactant for further coupling reactions.

Introducing the pyrazine ring in the middle of the isoindigo greatly influenced its absorption properties. The UV-vis absorption spectra of **BrIIG** and **BrPzIIG** are shown in Fig. 1 (a). **BrIIG** and **BrPzIIG** exhibit similar absorption features, with two major absorption bands located around 400 nm and 500 nm. The onset absorption edges of **BrIIG** and **BrPzIIG** are at 610 nm and 590 nm, corresponding to optical bandgaps of 2.03 eV and 2.10 eV, respectively. However, the absorbance of the **BrPzIIG** are nearly twice as that of the **BrIIG**, in the range between 300 nm and 600 nm. The maximum molar extinction coefficient for **BrIIG** is 17218 M⁻¹·cm⁻¹ at 400 nm and the maximum molar extinction coefficient for **BrPzIIG** is 29151 M⁻¹·cm⁻¹ at 405 nm. The much higher absorbance of **BrPzIIG** can be attributed to the extended conjugation¹³ due to the higher planarity. Fig. 1 (a) indicates that **BrPzIIG** is a much better light absorbing unit in the visible region compared with **BrIIG**. The absorption spectrum of **BrPzIIG** was simulated by time-dependent density functional theory (TD-DFT)¹⁴ (Fig. S1, ESI[†]) and the simulated spectrum is generally consistent with the experimental data. The simulation results indicate that the absorption band around 500 nm of **BrPzIIG** corresponds to the S₀-S₁ transition.

To further understand the relationship between the molecular structure and the frontier molecular orbital energy level, the highest occupied molecular orbital (HOMO) level and the lowest unoccupied molecular orbital (LUMO) level of **BrIIG** and **BrPzIIG** were calculated by density functional theory (DFT) at the B3LYP/6-311G (d, p) level¹⁴ and the alkyl chains were substituted by methyl group for simplicity. Fig. 2 (a) displays

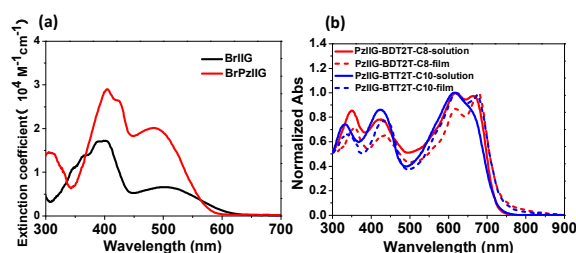


Fig. 1 (a) UV-vis absorption spectra of **BrIIG** and **BrPzIIG**; (b) Normalized absorption spectra of **PzIIG-BDT2TC8** and **PzIIG-BTT2TC10**.

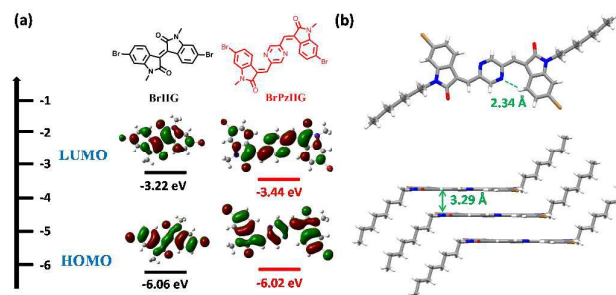
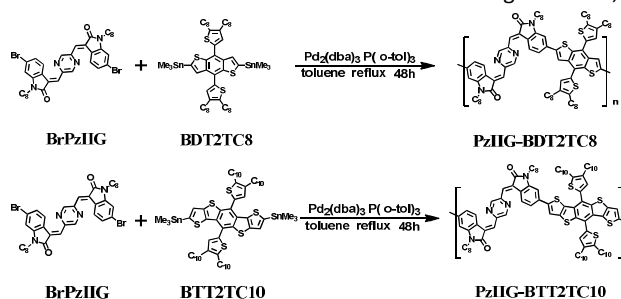


Fig. 2 (a) HOMO and LUMO energy levels based on DFT calculations at the B3LYP/6-311G (d, p) level of **BrIIG** and **BrPzIIG**; (b) Top view and side view single-crystal structure of **BrPzIIG**.

the calculated HOMO and LUMO energy levels of **BrIIG** and **BrPzIIG**. The HOMO and LUMO of **BrIIG** show relatively homogeneous distribution over the entire molecule. While the LUMO of **BrPzIIG** is largely distributed on the pyrazine ring and the HOMO of **BrPzIIG** is mainly localized on the indolone moieties. Meanwhile, the calculated HOMO and LUMO are -6.06 eV and -3.22 eV for **BrIIG**, and are -6.02 eV and -3.44 eV for **BrPzIIG**, respectively. Compared with **BrIIG**, the HOMO of **BrPzIIG** was slightly raised for 0.04 eV and the LUMO of **BrPzIIG** declined for 0.22 eV. The reduced band gap of **BrPzIIG** may be attributed to the electronegative nitrogen atom in the pyrazine ring. The cyclic voltammetry (CV) of **BrIIG** and **BrPzIIG** were measured (Fig. S2, ESI[†]), from which the HOMO and LUMO were estimated to be -5.77 eV and -3.66 eV for **BrIIG** and -5.69 eV and -3.68 eV for **BrPzIIG**, respectively.

The single crystal of **BrPzIIG** was obtained. Fig. 2 (b) displays the single crystal structure and the molecular packing of **BrPzIIG**. From the top view, an intramolecular hydrogen bonding between the nitrogen atom on the pyrazine ring and the hydrogen atom on the indolone can be observed. The length of the hydrogen bonding is 2.34 Å, which is accordance with the N-H hydrogen bonding distance. The side view confirms that the intramolecular hydrogen bonding makes the **PzIIG** very planar, which is in contrast to the twisted conformation of **IIG**. In the crystal, the **BrPzIIG** forms slipped face-to-face π-π stacked column with the plane distance of 3.29 Å. Both the close π-stacking and N-H hydrogen bonding may facilitate charge transfer in **PzIIG** based copolymers.

To assess the electron-withdrawing capability of the **PzIIG** unit, two benzodithiophene (**BDT**) derivatives, **BDT2TC8** and **BTT2TC10**, were selected as the electron-donating units. Using the **BrPzIIG** and the two **BDT** derivatives as starting materials,



Scheme 2 Synthetic routes of **PzIIG-BDT2TC8** and **PzIIG-BTT2TC10**.

$\text{Pd}_2(\text{dba})_3$ and $\text{P}(\text{o-tol})_3$ as catalysts, Stille-coupling polymerization in toluene gives two novel D-A conjugated copolymers: **PzIIIG-BDT2TC8** and **PzIIIG-BTT2TC10**. The synthetic routes of **PzIIIG-BDT2TC8** and **PzIIIG-BTT2TC10** are listed in Scheme 2 and the details of the synthetic process are described in ESI. The synthesized polymers were purified by a silica gel column (60 to 80 mesh) to afford metallic luster dark brown solid. The polymers exhibit good solubility in common organic solvents such as chloroform, toluene, chlorobenzene and *o*-dichlorobenzene. As determined by gel permeation chromatography (GPC) using THF as the eluent and monodisperse polystyrene as the standard, the **PzIIIG-BDT2TC8** has a number-average molecular weight (M_n) of 28.2 kDa and a polydispersity index (PDI) of 2.46, while the **PzIIIG-BTT2TC10** has a M_n of 23.5 kDa and a PDI of 2.18. Thermogravimetric analysis (TGA) shows excellent thermal stability of the **PzIIIG-BDT2TC8**, which shows a decomposition temperature (5% weight loss) over 352 °C; and the **PzIIIG-BTT2TC10** shows a decomposition temperature (5% weight loss) over 325 °C (Fig. S3, ESI†).

The UV-vis absorption spectra of **PzIIIG-BDT2TC8** and **PzIIIG-BTT2TC10** in CHCl_3 solutions and in thin films are displayed in Fig. 1 (b). The two polymers show broad absorption bands from 300 nm to 800 nm. The absorption bands in the high energy region from 300 nm to 500 nm are attributable to the delocalized excitonic $\pi-\pi^*$ transition. The broad bands in the low energy region from 500 nm to 800 nm are assigned to intramolecular charge transfer (ICT) interactions between the D and A units in the building blocks of polymers. The **PzIIIG-BDT2TC8** shows the maximum absorption wavelength (λ_{max}) at 620 nm and has a shoulder peak at 663 nm in solution. The **PzIIIG-BTT2TC10** displays the maximum absorption wavelength (λ_{max}) at 614 nm in solution. In solid films, the shoulder peak of **PzIIIG-BDT2TC8** turn into the maximum absorption peak and red-shifted 14 nm, while a new shoulder peak is appeared at 675 nm for **PzIIIG-BTT2TC10**. The red-shifted shoulder peak and new shoulder peak can be attributed to orderly $\pi-\pi$ stacking and shorter $\pi-\pi$ stacking distance in the solid state. The onset absorption edges as the thin films for **PzIIIG-BDT2TC8** and **PzIIIG-BTT2TC10** were at 762 nm and 756 nm, corresponding to optical bandgaps of 1.63 eV and 1.64 eV, respectively.

In order to investigate the electronic properties of **PzIIIG-**

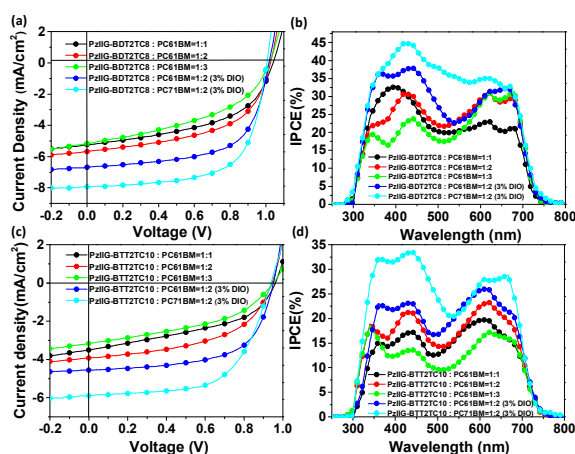


Fig. 3 (a) J–V curves and (b) IPCE curves of **PzIIIG-BDT2TC8-PC₆₁BM** and **PzIIIG-BDT2TC8-PC₇₁BM** based polymer solar cells under AM 1.5 G illumination, 100 mW/cm²; (c) J–V curves and (d) IPCE curves of **PzIIIG-BTT2TC10-PC₆₁BM** and **PzIIIG-BTT2TC10-PC₇₁BM** based polymer solar cells under AM 1.5 G illumination, 100 mW/cm².

BDT2TC8 and **PzIIIG-BTT2TC10**, molecular simulations by DFT model were performed on their dimers with methyl substituted alkyl chains for simplicity (Fig. S4, ESI†).¹⁴ The two dimers possess the same values of the HOMO and LUMO energy levels (-5.06 eV for HOMO and -3.06 eV for LUMO). Moreover, both dimers have similar HOMO and LUMO distribution. The HOMO of two dimers mainly locates at the **BDT2TC8** and **BTT2TC10** moieties and LUMO mostly locates around the **PzIIIG** moieties, indicating strong ICT. The HOMO and LUMO energy levels of the two polymers were also estimated by CV (Fig. S2, ESI†). The HOMO and LUMO levels of **PzIIIG-BDT2TC8** are estimated to be -5.48 eV and -3.64 eV, respectively. While the HOMO and LUMO levels of **PzIIIG-BTT2TC10** are -5.40 eV and -3.58 eV, respectively. According to previous literatures, a conductive polymer is air stable if the HOMO energy level is below the air oxidation threshold (ca. -5.27 eV).^{15,16} Therefore, the measured HOMO energy levels of **PzIIIG-BDT2TC8** and **PzIIIG-BTT2TC10** indicate that these two polymers are air stable. Besides, the low-lying HOMO energy levels are also beneficial for high V_{oc} in the PSCs device.¹⁵ The LUMO energy levels of **PzIIIG-BDT2TC8** (-3.64 eV) and **PzIIIG-BTT2TC10** (-3.58 eV) are 0.3 eV higher than fullerene derivatives (Fig. S2, ESI†), which afford

Table 1 The photovoltaic parameters of the solar cells from **PzIIIG-BDT2TC8** and **PzIIIG-BTT2TC10**

Active layer	Additive	V_{oc} (V)	J_{sc} (mA/cm ²)	FF (%)	PCE (%)
PzIIIG-BDT2TC8:PC ₆₁ BM=1:1	without	1.04	5.23	50.28	2.74
PzIIIG-BDT2TC8:PC ₆₁ BM=1:2	without	1.03	5.68	53.39	3.12
PzIIIG-BDT2TC8:PC ₆₁ BM=1:3	without	1.02	5.16	44.26	2.33
PzIIIG-BDT2TC8:PC ₆₁ BM=1:2	3% DIO	1.02	6.68	62.18	4.24
PzIIIG-BDT2TC8:PC ₇₁ BM=1:2	3% DIO	1.01	7.93	65.63	5.26
PzIIIG-BTT2TC10:PC ₆₁ BM=1:1	without	0.96	3.50	44.35	1.49
PzIIIG-BTT2TC10:PC ₆₁ BM=1:2	without	0.95	3.92	50.86	1.89
PzIIIG-BTT2TC10:PC ₆₁ BM=1:3	without	0.95	3.16	43.80	1.31
PzIIIG-BTT2TC10:PC ₆₁ BM=1:2	3% DIO	0.95	4.55	61.61	2.66
PzIIIG-BTT2TC10:PC ₇₁ BM=1:2	3% DIO	0.94	5.89	60.78	3.36

sufficient driving force to transfer charge from polymers to PCBM.

Bulk heterojunction (BHJ) PSCs were fabricated in an inverted device structure of ITO / PFN / polymer : PC₆₁BM / MoO₃ / Ag. The two polymers have good solubility in chlorobenzene (CB), so blended polymers with PC₆₁BM at different weight ratios in CB at 1:1, 1:2 and 1:3 were tested to optimize the devices performance. 1,8- diiodooctane (DIO) was used as the additives and the films were annealed at 120 °C to obtain the optimal phase separation. The J–V curves and the incident photon-to-current conversion efficiency (IPCE) curves of **PzIIG-BDT2TC8** and **PzIIG-BTT2TC10** based PSCs are displayed in Fig. 3. The **PzIIG-BDT2TC8**-PC₆₁BM gave the best device performance based on the weight ratio at 1:2 (w/w), DIO 3 % (wt.) in CB and annealing at 120 °C, which exhibited a PCE of 4.24 % with a V_{oc} of 1.02 V, a J_{sc} of 6.68 mA / cm², and a FF of 62.18 %. The **PzIIG-BTT2TC10**-PC₆₁BM gave the best device performance based on the weight ratio at 1:2 (w/w), DIO 3 % (wt.) in CB and annealing at 120 °C, which exhibited a PCE of 2.66 % with a V_{oc} of 0.95 V, a J_{sc} of 4.55 mA / cm², and a FF of 61.61 %. As PC₇₁BM possess much stronger absorbance in the visible region compare with PC₆₁BM, PC₇₁BM was used to fabricate PSCs device at the same conditions for performance optimization.¹⁷ The **PzIIG-BDT2TC8**-PC₇₁BM based device exhibited a PCE of 5.26 % with a V_{oc} of 1.01 V, a J_{sc} of 7.93 mA / cm², and a FF of 65.63 %. The **PzIIG-BTT2TC10**-PC₇₁BM based device exhibited a PCE of 3.36 % with a V_{oc} of 0.94 V, a J_{sc} of 5.89 mA / cm², and a FF of 60.78 %. In comparison, Zhang has reported that **IIG** and **BDT** based D-A copolymer gave a PCE of 4.02 %, which has very similar molecular structure to **PzIIG-BDT2TC8**.¹⁸ It suggests that using the **PzIIG** to construct D-A copolymer may be an effective way to obtain high performance PSCs. The details of PSCs performance for **PzIIG-BDT2TC8** and **PzIIG-BTT2TC10** are listed in Table 1. The corresponding IPCEs of the polymer-based solar cell devices (Fig. 3 (b) and Fig. 3 (d)) were measured, which matched well with the results obtained from the J–V characteristics. High V_{oc} over 1.0 V is not easy to obtain in the PSCs. The two polymers based PSCs devices exhibited high open circuit voltage, which can be attributed to the deep HOMO energy levels (-5.48 eV for **PzIIG-BDT2TC8** and -5.40 eV for **PzIIG-BTT2TC10**) of the polymers (Fig. S2, ESI[†]). The HOMO energy level of **PzIIG-BDT2TC8** is 0.08 eV lower than that of the **PzIIG-BTT2TC10**, which may explain the higher V_{oc} of the **PzIIG-BDT2TC8** based PSCs device. The hole mobilities were measured by the space charge limited current (SCLC) method (Fig. S5, ESI[†]), which gave moderate hole mobilities of 6.57x10⁻⁵ cm² v⁻¹ s⁻¹ for **PzIIG-BDT2TC8** and 5.92x10⁻⁵ cm² v⁻¹ s⁻¹ for **PzIIG-BTT2TC10**.¹⁹

The thin film morphologies of the polymers blend were characterized by tapping-mode Atomic Force Microscope (AFM) (Fig. S6, ESI[†]). Both polymers blend with DIO show smaller domain size compared with the polymers blend without DIO, which result in improved microphase separation in the films. The root-mean-square (RMS) roughness was 5.96 nm and 6.45 nm for the **PzIIG-BDT2TC8** blend with DIO and the **PzIIG-BTT2TC10** blend with DIO, respectively. This result suggests the **PzIIG-BDT2TC8** was more homogeneous with better phase separation compared with **PzIIG-BTT2TC10**, and the morphology of the **PzIIG-BDT2TC8** based film facilitates better device performance. Although adding DIO can effectively improve the morphology of the films, the inhomogeneity of the films and big RMS in the AFM images indicating poor

morphology of the films, which may explain the relatively low photocurrent. Therefore, the PCEs of the two polymers can be further enhanced by improving the film morphology.

In summary, we have designed and synthesized a novel electron acceptor structure, **PzIIG**. The introduction of pyrazine ring in the middle of isoindigo induces intramolecular hydrogen bonding and high molar extinction coefficient. Using the **PzIIG** as electron withdrawing unit we constructed two D-A conjugated polymers: **PzIIG-BDT2TC8** and **PzIIG-BTT2TC10**. Inverted polymer solar cell devices based on **PzIIG-BDT2TC8** and **PzIIG-BTT2TC10** exhibited PCEs of 5.26 % and 3.36 %, respectively. It is noted that the PSCs based on **PzIIG-BDT2TC8** exhibit high V_{oc} above 1.0 V. Further improvement in PSCs performance may include optimizing the device preparation conditions through enhancing the morphology of active layers such as solvent vapor annealing (SVA) methods and selection of the additives. Design and synthesis of **PzIIG** containing D-A conjugated polymers with other donor units and different side chains are currently underway. Our results indicate that **PzIIG** is a promising building block for constructing D-A conjugated copolymers for optoelectronic applications.

This work is supported by National Natural Science Foundation of China (NSFC. 51525303, 21233001, 21572086), Fundamental Research Funds for the Central Universities and the 111 Project.

Notes and reference

1. C. Wang, H. Dong, W. Hu, Y. Liu and D. Zhu, *Chem. Rev.*, 2012, **112**, 2208-2267.
2. L. Lu, T. Zheng, Q. Wu, A. M. Schneider, D. Zhao and L. Yu, *Chem. Rev.*, 2015, **115**, 12666-12731.
3. E. Wang, Z. Ma, Z. Zhang, K. Vandewal, P. Henriksson, O. Inganäs, F. Zhang and M. R. Andersson, *J. Am. Chem. Soc.*, 2011, **133**, 14244-14247.
4. C. Dou, X. Long, Z. Ding, Z. Xie, J. Liu and L. Wang, *Angew. Chem. Int. Ed.*, 2016, **55**, 1436-1440.
5. X. Long, Z. Ding, C. Dou, J. Zhang, J. Liu and L. Wang, *Adv. Mater.*, 2016, **28**, 6504-6508.
6. W. Li, W. S. C. Roelofs, M. M. Wienk and R. A. J. Janssen, *J. Am. Chem. Soc.*, 2012, **134**, 13787-13795.
7. T. Lei, J.-Y. Wang and J. Pei, *Acc. Chem. Res.*, 2014, **47**, 1117-1126.
8. C. Lu, H.-C. Chen, W.-T. Chuang, Y.-H. Hsu, W.-C. Chen and P.-T. Chou, *Chem. Mater.*, 2015, **27**, 6837-6847.
9. G. K. Dutta, A. R. Han, J. Lee, Y. Kim, J. H. Oh and C. Yang, *Adv. Funct. Mater.*, 2013, **23**, 5317-5325.
10. R. S. Ashraf, A. J. Kronemeijer, D. I. James, H. Sirringhaus and I. McCulloch, *Chem. Commun.*, 2012, **48**, 3939-3941.
11. G. Kim, S.-J. Kang, G. K. Dutta, Y.-K. Han, T. J. Shin, Y.-Y. Noh and C. Yang, *J. Am. Chem. Soc.*, 2014, **136**, 9477-9483.
12. S. K. Das and J. Frey, *Tetrahedron Lett.*, 2012, **53**, 3869-3872.
13. S. Li, Z. Yuan, J. Yuan, P. Deng, Q. Zhang and B. Sun, *J. Mater. Chem. A*, 2014, **2**, 5427-5433.
14. M. J. F. R. A. Gaussian, G. W. Trucks, H. B. Schlegel, et al., *Gaussian, Inc., Wallingford, CT*, 2009.
15. N. Blouin, A. Michaud, D. Gendron, S. Wakim, E. Blair, R. Neagu-Plesu, M. Belletête, G. Durocher, Y. Tao and M. Leclerc, *J. Am. Chem. Soc.*, 2008, **130**, 732-742.
16. D. M. de Leeuw, M. M. J. Simenon, A. R. Brown and R. E. F. Einerhand, *Synth. Met.*, 1997, **87**, 53-59.
17. Y. He and Y. Li, *Phys. Chem. Chem. Phys.*, 2011, **13**, 1970-1983.
18. K. Cao, Z. Wu, S. Li, B. Sun, G. Zhang and Q. Zhang, *J. Polym. Sci. Pol. Chem.*, 2013, **51**, 94-100.
19. G. Zhang, Y. Fu, Z. Xie and Q. Zhang, *Macromolecules*, 2011, **44**, 1414-1420.